

Supporting Information

Halosilane Triggers Anodic Silanization and Cathodic Redox for Stable and Efficient Lithium-O₂ Batteries

Xiaohui Zhao,^{ab} Zhuang Sun,^a Zhenguo Yao,^a and Tao Zhang^{*ab}

Abstract: Fundamental challenges with the inefficient decomposition of Li₂O₂, the undesirable “shuttled effects” reactions of redox mediators (RMs) with Li, and the anodic corrosion from electrolyte attacks have seriously hindered the development of Li-O₂ batteries. We create and study a self-defense indissoluble LiOSi(CH₃)₃ layer based on halosilane (iodotrimethylsilane, TMSI) tethered to the rational designed oxygen-pretreated-Li (OPL) anode to overcome the most above stubborn challenges. The silanization layer is shown to protect the Li anode against parasitic reactions and also stabilize Li electrodeposition during cell cycling. Iodine species self-released during the anchoring reaction can function as RMs at the cathode, reducing the charge overpotential. Finally, the combination of self-defense and self-release approaches through solely inducing halosilane into liquid electrolytes endows lithium-O₂ batteries with excellent cycling stability and electrical energy efficiency.

^aThe State Key Lab of High Performance Ceramics and Superfine microstructure, Shanghai Institute of Ceramics, Chinese Academy of Sciences, 1295 Dingxi Road, Shanghai, 200050, P. R. China.

^bCenter of Materials Science and Optoelectronics Engineering, University of Chinese Academy of Sciences, Beijing 100049, PR China.

*Corresponding Author: E-mail: taozhang@mail.sic.ac.cn

DOI: 10.1039/x0xx00000x

Table of Contents

1.0 Experimental Section	3
1.1 DMSO-based electrolyte.....	3
1.2 MWCNT cathodes	3
1.3 Li anode	3
1.4 Assembling Li-O ₂ coin cell and Li-Li symmetric cell.....	3
2.0 Electrochemical analysis and material characterization	4
2.1 Electrochemical measurement	4
2.2 SEM observation and EDS analysis	4
2.3 FTIR analysis	4
2.4 XPS analysis	5
2.5 XRD measurement.....	5
3.0 Figures	6
Figure S1. SEM images of Li metal surface before and after pretreatment.	6
Figure S2. FTIR spectra of Li metal surface before and after pretreatment.	7
Figure S3. a) The FTIR spectra of pretreated Li metal surface with the addition of TMSI, b) the schematic illustration of the in-situ FTIR measurements and c) the headspace gas chromatography of lithium anode in TMSI-containing Li-O ₂ batteries after 5 cycles.....	8
Figure S4. Elemental mappings of the cross section of Li anode in a battery with 50mM LiI.	10
Figure S5. EIS analysis corresponding to <i>Fig. 1k,l</i>	11
Figure S6. XRD patterns of the cathode product after discharging and charging in the cells with the addition of TMSI.....	12
Figure S7. The electrochemical impedance spectra of Li-O ₂ cells with TMSI	13
Figure S8. The cross-section morphologies of Li anode in TMSI-containing Li-O ₂ batteries.....	14
Figure S9. (a) S 2p, (b) Cl 2p XPS spectra of Li anode surface in batteries with 50mM LiI.....	15
Table S1 The reaction energy of corresponding reactions in DMSO-based Li-O ₂ batteries.....	16

1.0 Experimental Section

1.1 DMSO-based electrolyte

A DMSO-based electrolyte consists of 1M LiClO₄ in pure DMSO. 50mM TMSI and 50mM LiI were added into the electrolyte as additive, respectively.

1.2 MWCNT cathodes

Multi-wall carbon nanotubes (MWCNTs, XFNANO, 8-15nm) and polyvinylidene fluoride (PVDF) were mixed with weight ratio of 9:1 to form a homogenous slurry with N-methyl-2-pyrrolidone, and then the slurry was brushed onto carbon paper current collector, and vacuum dried at 80 °C for 24h, The loading area was 0.385 cm² (7 mm in diameter) and the loading weight of MWCNT was $\approx 0.5 \text{ mg cm}^{-2}$.

1.3 Li anode

The Li foil of thickness 0.2 mm was cut into discs of 12 mm in diameter, and then the pristine Li were washed by tetrahydrofuran (THF) for 5 minutes. After dried, the THF-treated Li were put into a bottle with pure oxygen and trace quantities of water (<500 ppm), sealed and standing for 10h, and the oxygen-pretreated-Li (OPL) was obtained.

1.4 Assembling Li-O₂ coin cell and Li-Li symmetric cell

The batteries were assembled in a glove box filled with high-purity argon (O₂ and H₂O < 0.1 ppm). Li-O₂ cells were assembled with cathode of MWCNT, separators of Waterman GF/C glass fiber, 100 μL DMSO-based electrolyte, and anode of OPL in a coin cell (CR2032 type, with holes). The cell was placed in pure oxygen and standing for 6 h before testing. Symmetric Li metal coin cells (2025 type) were assembled with two OPL, separated by a Waterman GF/C glass fiber separator. The amount of the electrolyte (1M LiClO₄ in DMSO with or without 50mM TMSI) in each cell was 100 μL . The current density of cells were fixed at 0.7 mA cm⁻², cells were firstly discharged for 1.5 h and then charged for the same time with a cut-off voltage at $\pm 0.5 \text{ V}$ versus Li/Li⁺.

2.0 Electrochemical analysis and material characterization

2.1 Electrochemical measurement

To measure the electrochemical capacity and cycle life of the working electrodes, the assembled cells were galvanostatically charged and discharged using LAND electrochemical testing system in an oxygen-filled glovebox. The cycling test was conducted with capacity limited at 1000 mAh g⁻¹ at a current densities of 500 mA g⁻¹. For Li-Li symmetric cells, the discharge time was set at 1.5 hours with a cutoff voltage of -0.5 V at 0.7 mA cm⁻², whereas the charge cutoff voltage was 0.5 V with the same current density and time. Cyclic voltammetry (CV) was performed on Bio-Logic VSP between 2.0V and 4.2V at a scan rate of 0.1 mV s⁻¹. Electrochemical impedance spectroscopy (EIS) was carried out with amplitude of 10 mV over the frequency range from 1.0 × 10⁶ Hz to 0.1 Hz.

2.2 SEM observation and EDS analysis

The field emission scanning electron microscope (FE-SEM, SU8220) was used for observation of Li anode and EDS mapping analysis. The cells after cycling were disassembled in argon-filled glove box, the Li anode obtained were rinsed with 1, 2-dimethoxyethane (anhydrous, Sigma) and then dried for 2h before further analysis. During transferring process before characterizations, all samples were sealed in a transporter to avoid contact with air.

2.3 FTIR analysis

The pristine Li, THF-treated Li, THF/O₂-pretreated Li and cycled Li anodes were prepared for Fourier transform infrared (FTIR) analysis on a Thermo Fisher Scientific instrument of FT/IR-Nicolet

iS5 from 4000 to 500 cm^{-1} . The Li anodes of TMSI-containing cells were disassembled after cycling, washed with 1, 2-dimethoxyethane (anhydrous, Sigma) and then dried for 2h.

2.4 XPS analysis

The components of protective layer on the lithium anode were detected by X-ray photoelectron spectroscopy (XPS, ESCALAB250) test. The cells after cycling were disassembled and the obtained anode sample were washed with 1, 2-dimethoxyethane and then dried for 2h. A sealed transfer system was employed to transfer samples from the glovebox to XPS system.

2.5 XRD measurement

After discharging and recharging, the MWCNT cathode of cells with 50mM TMSI were collected for X-ray diffraction (XRD) measurement, respectively. The XRD patterns were collected on a BRUKER AXS GMBH (D8 ADVANCE) machine with $\text{Cu K}\alpha$ radiation at the angle range of 10-80°.

3.0 Figures

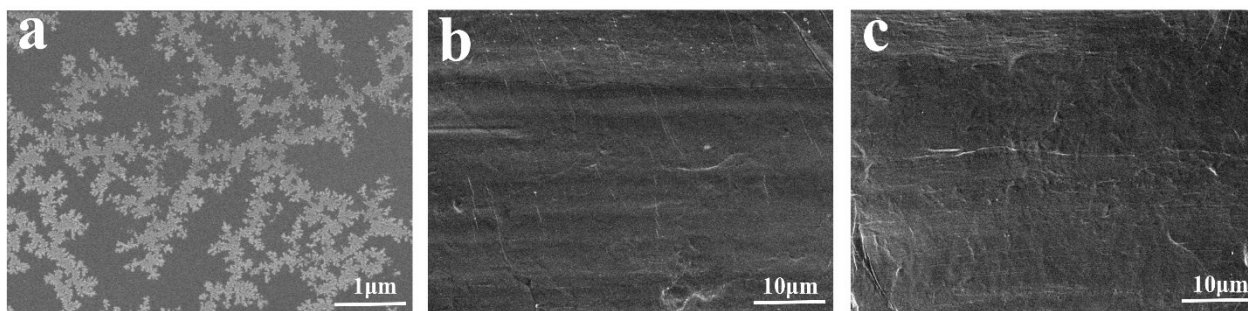


Figure S1. SEM images of Li metal surface before and after pretreatment. (a) pristine Li, (b) after treatment of THF and (c) after treatment of THF/O₂ (H₂O<500 ppm).

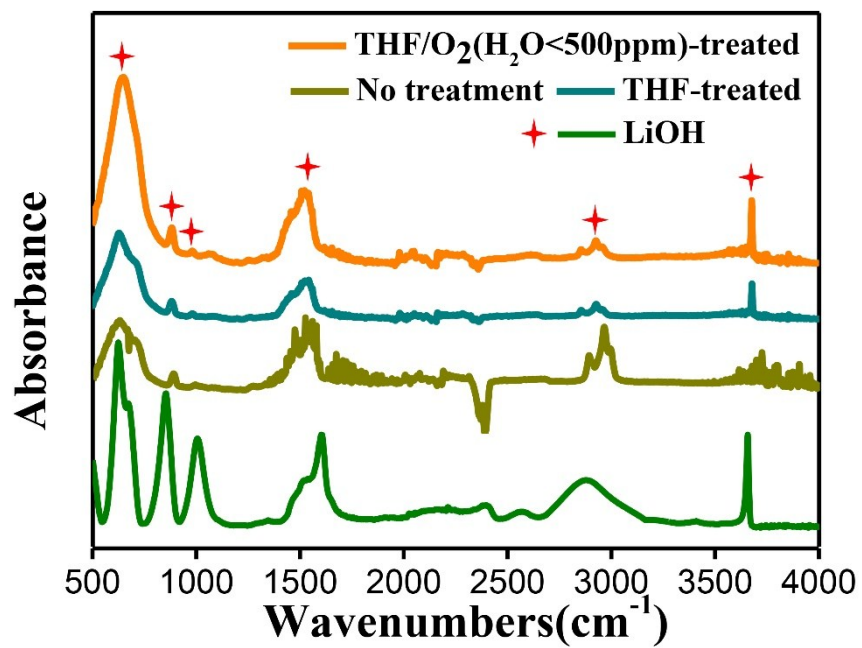


Figure S2. FTIR spectra of Li metal surface before and after pretreatment.

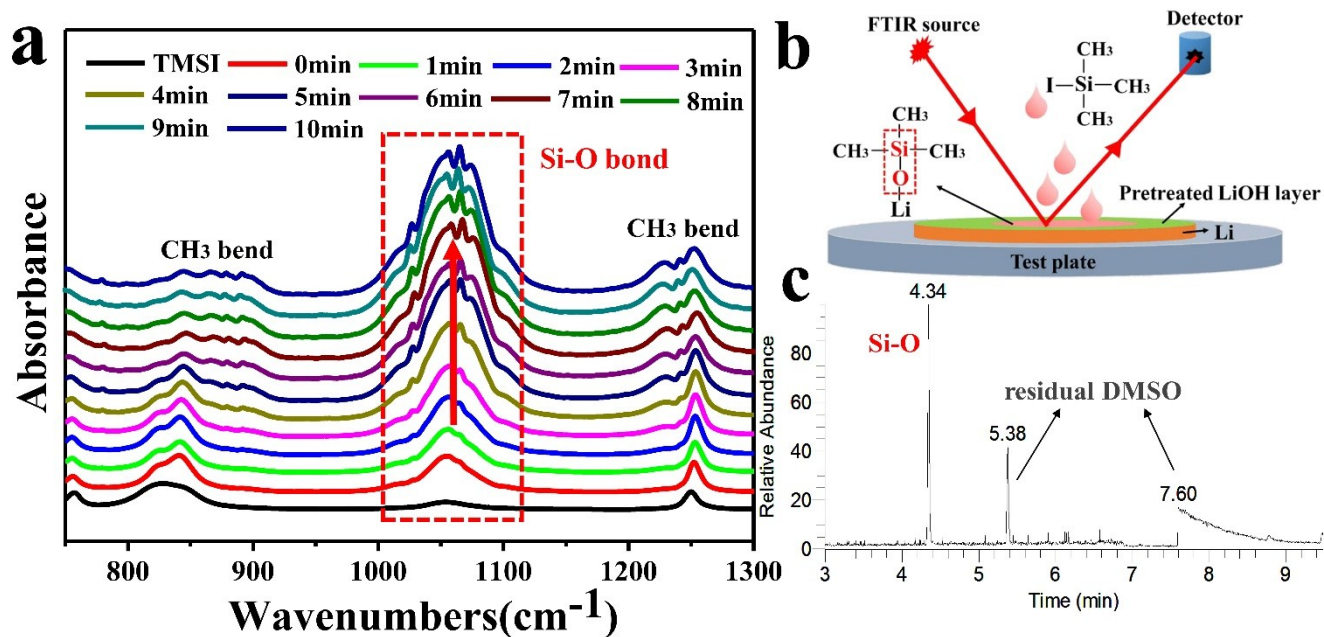


Figure S3. a) The FTIR spectra of pretreated Li metal surface with the addition of TMSI, b) the schematic illustration of the in-situ FTIR measurements and c) the headspace gas chromatography of lithium anode in TMSI-containing Li-O₂ batteries after 5 cycles.

The in-situ FTIR measurements were conducted in a glove box filled with argon, prior to experiments the lithium disc was pretreated to obtain a thin LiOH layer on Li surface. Then, the FTIR signals were gathered every minutes after dropping 20 μ L TMSI, onto the pretreated Li (as shown in figure S3b). The designed in-situ FTIR measurements provide the possibility to directly observe the spectra changes as the time prolongs (figure S3a). Firstly, before contacting with the pretreated Li foil, the liquid droplets show obvious CH₃-bends, which may be from the TMSI, and weak Si-O bond, which may be from the inevitably contamination of TMSI in the transfer process of the reagents. It is worth noting that the intensity of Si-O peak increased instantaneously as the droplets of TMSI touched the pretreated Li surface (0 min), illustrating the spontaneous reaction of TMSI and LiOH and forming numerous covalent Si-O bonds. Secondly, the intensity of Si-O bonds increased gradually as time

prolongs (0 to 10 min), which may be due to the constant formation of the protective $\text{LiOSi}(\text{CH}_3)_3$ surface layer until it become stabilized. Finally, the Li foil disassembled from the Li- O_2 battery with TMSI after 5 cycles was sealed, and further characterized by the ex-situ headspace gas chromatography, as shown in the figure S3c, the existent of Si-O bond further verified the reaction products from the coating reaction process: $\text{LiOH} + \text{ISi}(\text{CH}_3)_3 \rightarrow \text{LiOSi}(\text{CH}_3)_3 + \text{HI}$.

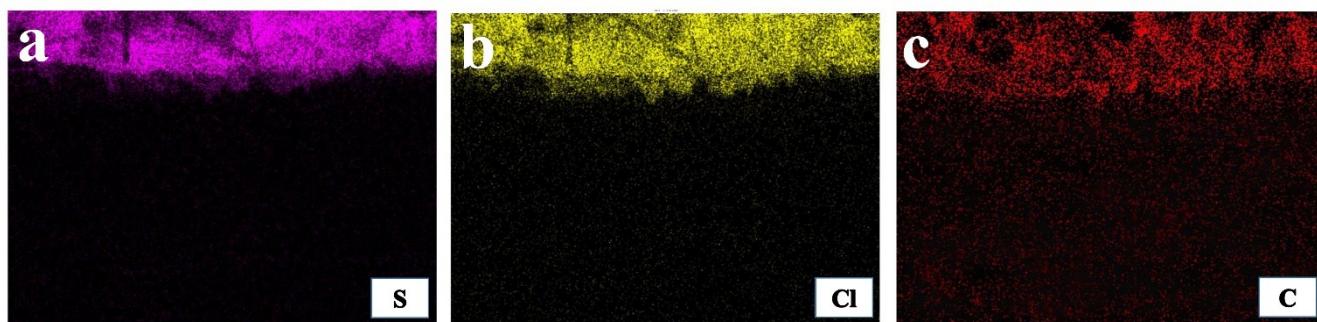


Figure S4. Elemental mappings of the cross section of Li anode in a battery with 50mM Lil. (a) Sulfur, (b) Chlorine and (c) Carbon

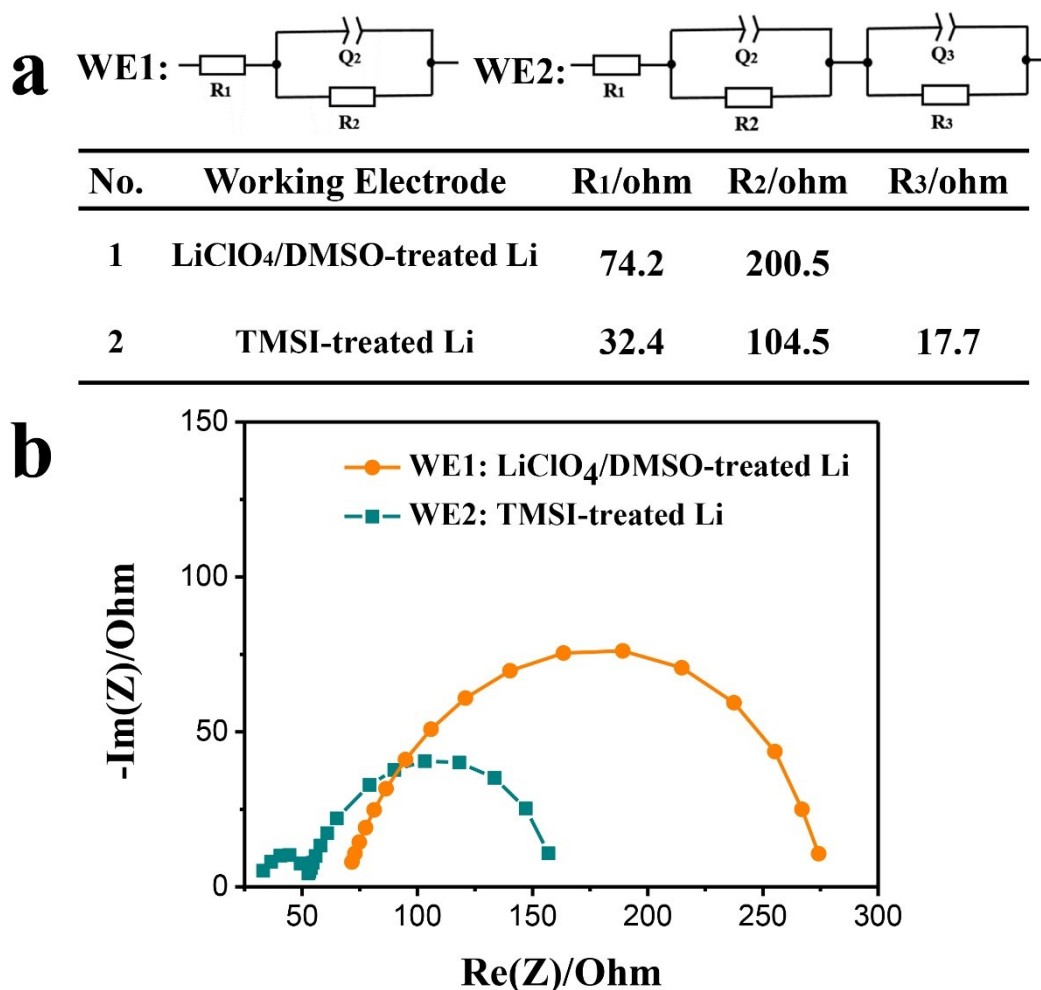


Figure S5. EIS analysis corresponding to Fig. 1k,l. EIS analysis with (a) equivalent circuit model and fitting parameters, (b) Nyquist plots of fitted results.

For the LiClO₄/DMSO-treated Li electrode (WE1), only one semicircle can be observed in the EIS spectra, which represents the charge-transfer resistance of Li/electrolyte interface. By contrast, two semicircles are exhibited in the cell with TMSI-treated Li electrode (WE2). It is worth pointing out that the low-frequency semicircle appears in the case of TMSI-treated Li, which indicates the existence of a protective layer on the Li electrode. Meanwhile, the smaller charge-transfer resistance of WE2 (104.5 ohm) compared with the WE1 (200.5 ohm), implying that the thin film formed on the Li electrode can suppress the parasitic reaction in cycling process.

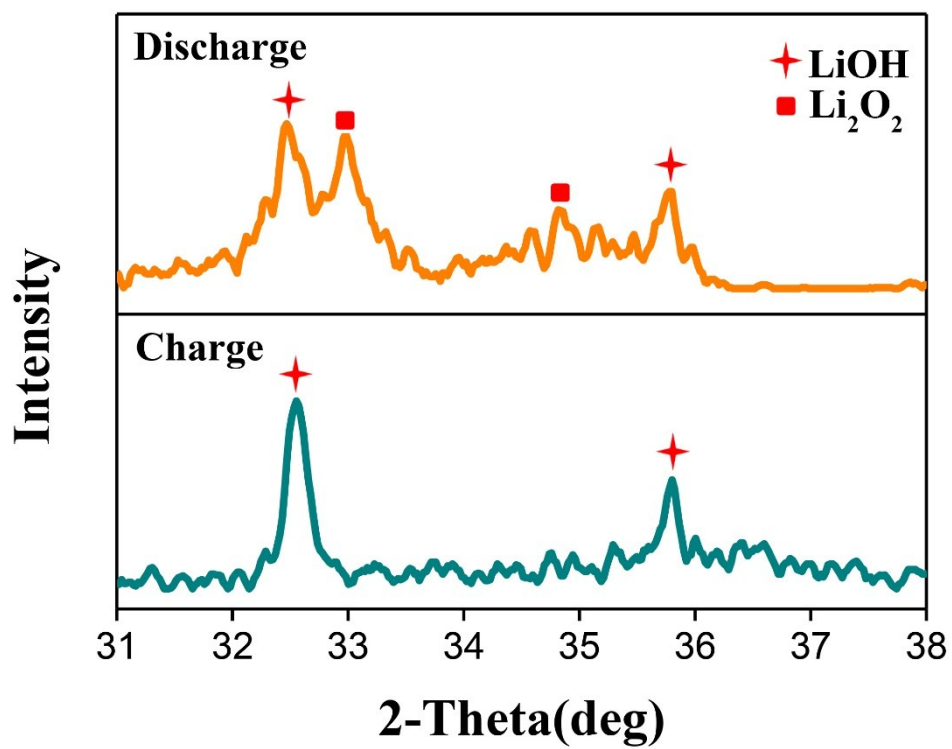


Figure S6. XRD patterns of the cathode product after discharging and charging in the cells with the addition of TMSI.

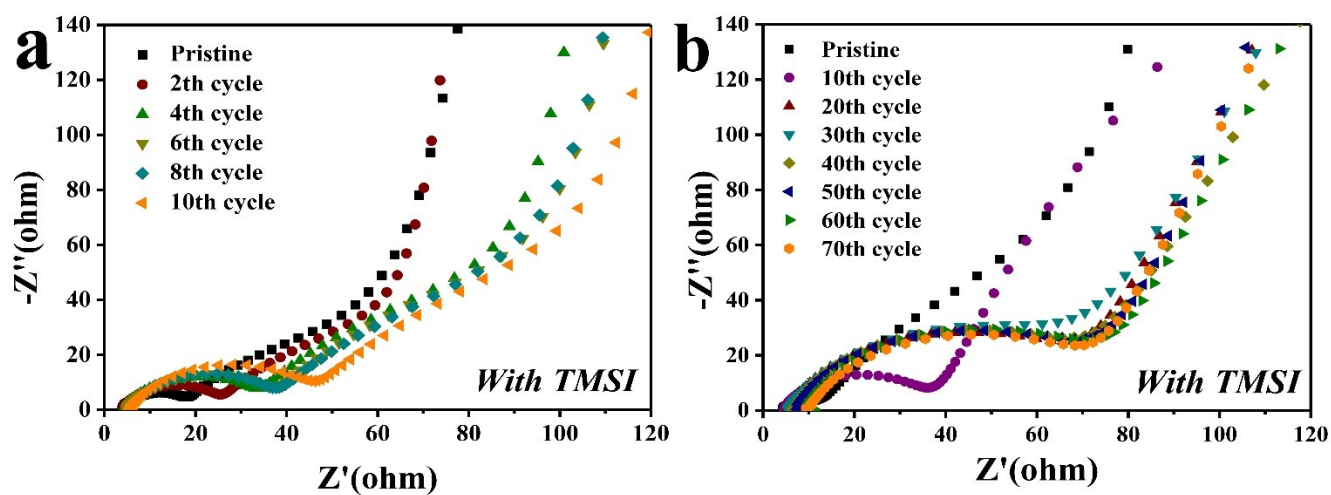


Figure S7. The electrochemical impedance spectra of Li-O₂ cells with TMSI a) at the first 10 cycles and b) at every 10 cycles.

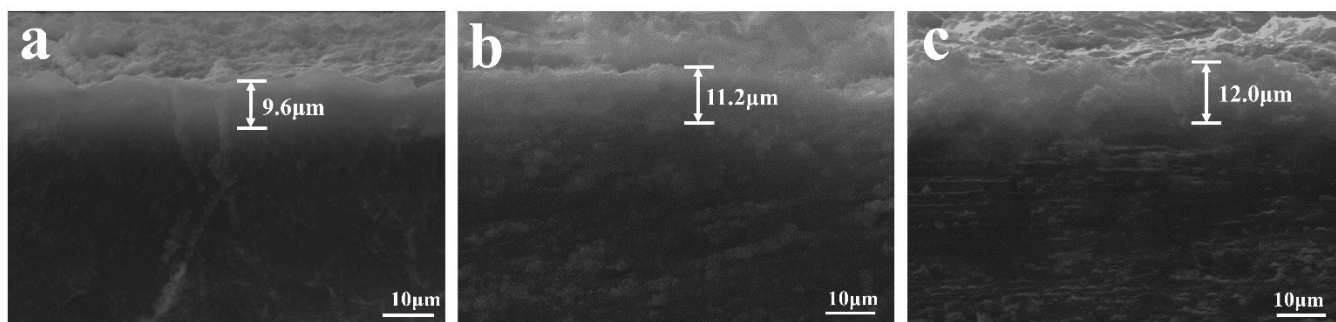


Figure S8. The cross-section morphologies of Li anode in TMSI-containing Li-O₂ batteries after a) 1 cycle, b) 20 cycles and c) 50 cycles.

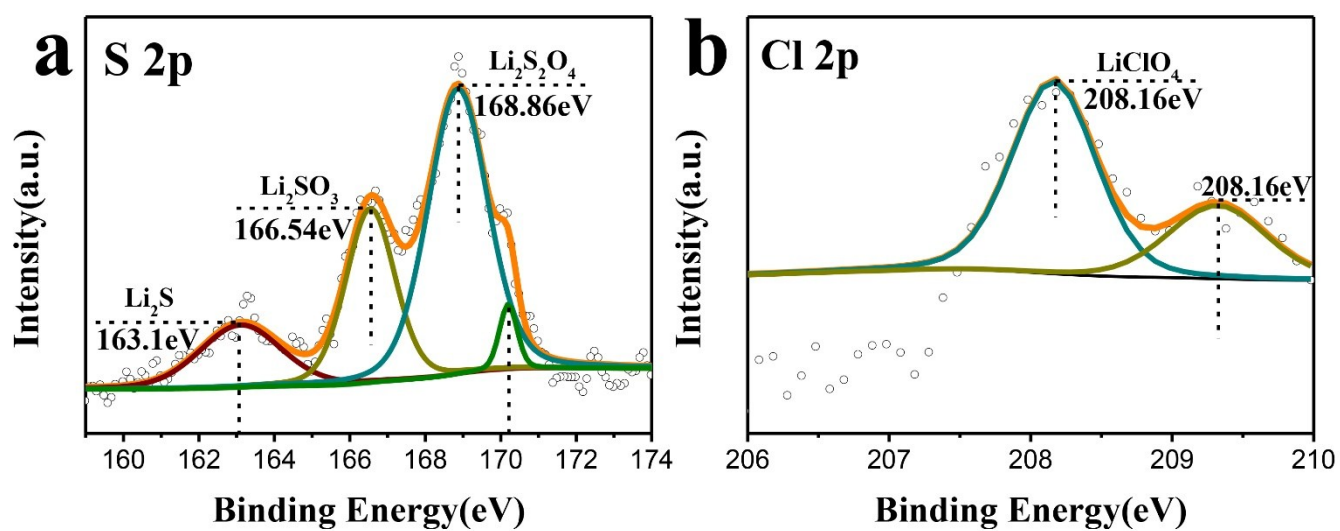


Figure S9. (a) S 2p, (b) Cl 2p XPS spectra of Li anode surface in batteries with 50mM LiI.

Table S1 The reaction energy of corresponding reactions in DMSO-based Li-O₂ batteries.

Reaction equation	Reaction energy/eV
$\text{CH}_3\text{-S=O-CH}_3 + 2\text{Li} \rightarrow \text{CH}_3\text{-S-CH}_3 + \text{Li}_2\text{O}$	-4.35838193
$\text{LiClO}_4 + 8\text{Li} \rightarrow \text{LiCl} + 4\text{Li}_2\text{O}$	-22.5249354
$\text{LiClO}_4 + \text{LiOSi}(\text{CH}_3)_3$	Nonspontaneous
$\text{CH}_3\text{-S=O-CH}_3 + \text{LiOSi}(\text{CH}_3)_3$	Nonspontaneous
$\text{I}_3^- + \text{LiOSi}(\text{CH}_3)_3$	Nonspontaneous

The reaction energy was estimated by first-principles computations based on density functional theory (DFT). The Vienna ab initio simulation package (VASP)^[1] with the projector-augmented wave (PAW)^[2] and Perdew-Burke-Ernzerhof (PBE) parametrization of the generalized gradient approximation (GGA)^[3] were used as pseudopotentials and exchange-correlation functional, respectively. A 500 eV kinetic energy cutoff was employed in all the computations. As for the calculations of molecules, the molecules were placed into a $25 \times 25 \times 25 \text{ \AA}^3$ lattice and a gamma Monkhorst-Pack k-point sampling scheme was adopted after a careful convergence test. The energy convergence criteria were set in the order of 10^{-5} eV and the structures were relaxed until the force on each atom was less than 0.05 eV \AA^{-1} . The reaction energy was defined as the energy difference between resultants and reactants. And the higher energy of the resultants compared with the reactants indicates the nonspontaneous reaction.

- 1 G. Kresse, J. Furthmuller, *Comp Mater Sci* **1996**, 6, 15-50.
- 2 P. E. Blochl, *Phys Rev B* **1994**, 50, 17953-17979.
- 3 J. P. Perdew, K. Burke, M. Ernzerhof, *Phys Rev Lett* **1996**, 77, 3865-3868.